

Numerical Modeling, Thermomechanical Testing, and NDE Procedures for Prediction of Microcracking Induced Permeability of Cryogenic Composites

Jae Noh, John Whitcomb*
Bongtaek Oh, Dimitris Lagoudas
Konstantin Maslov, Atul Ganpatye, Vikram Kinra

Center for Mechanics of Composites
Aerospace Engineering Department
Texas A&M University
College Station, TX 77843-3141

INTRODUCTION

Reusable Space Vehicles will include light cryogenic composite fuel tanks that must not leak excessively even after multiple launches. Damage in cryogenic composite fuel tanks induced during manufacturing and advanced by thermomechanical cycling can accelerate leakage of the propellant. Whether the leakage exceeds tolerable levels depends on many factors, including pressure gradients, microcrack density, other damage such as delamination, connectivity of the cracks, residual stresses from manufacture, service-induced stresses from thermal and mechanical loads, and composite lay-up. Although it is critical to experimentally characterize permeability during various thermal and mechanical load histories, optimal design depends on having analytical models that can predict the effect of various parameters on performance. Our broad goal is to develop such models that are experimentally validated by destructive and non-destructive evaluation means.

The literature provides limited studies on the mechanical performance of and damage development in polymer matrix composites operating at cryogenic temperature. Adams, *et al.* [1] investigated thermally induced matrix cracking for graphite/epoxy cross-ply laminates exposed to thermal cycles (-250°F to 250°F). They found the crack density increases with thermal cycles for all laminate configurations tested. Kessler *et al.* [2] have cycled carbon/polymer composites with a combined cycle to simulate the operating environment of the X-33's composites fuel tanks. A single cycle consisted of a cool-down from 300K to 20K, a heat-up 400K, and then back to 300K. There were no microcracks present or apparent loss in stiffness or strength properties after 10 cycles in quasi-isotropic laminates which are identical to the material used on the X-33. Different types of the cross-ply and quasi-isotropic laminates were thermo-mechanically cycled to examine the initiation and development of damage [3-5]. The literature survey suggests that the detailed study on the damage characterization for cross- and angle-ply laminates must be performed for various loading histories. The current study will include a comparison of damage development in accordance with loading history.

There are a few recent studies that investigated the possibility of predicting leakage of cryogenic fuel from composite tanks. Some experiments with measurement of the leak rate through polymer composite are found in the literature [2,6-10]. McManus, *et al.* presented analytical and experimental results for crack induced permeability under cryogenic conditions [7,8]. Kumazawa conducted numerical analysis to predict the leak rates at cryogenic temperature [9]. They took into account the influences of both thermal contraction and reduced molecular dynamics. They developed an analytical method to quantitatively predict the leakage based on the simple assumption that there is a relationship between

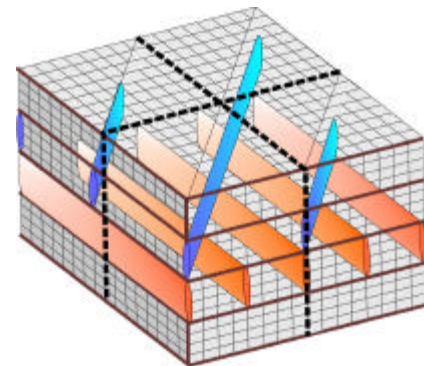


Figure 1. Angle ply laminate with transverse matrix cracks

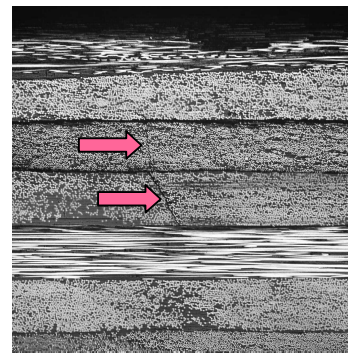


Figure 2. Micrograph showing cracks in a laminate

* E-mail: whit@aero.tamu.edu Phone: 979-845-4006

leakage and opening displacement of matrix cracks. The study on the leakage at cryogenic condition is at a preliminary stage. Many factors (damage state, opening displacement, permeability, etc) affecting the leakage must be carefully examined to develop an analytical model and compare with experimental results.

Since the amount of leakage will increase with crack opening volume (COV), it is essential that we understand crack opening and factors that affect the crack opening. One of objectives in the current work is to show that the crack opening volume can be directly related to the degradation behavior of the effective moduli of a cracked ply. The effect of damage on effective moduli has been studied extensively [11-15]. A simple expression for the COV will be derived based on the modulus reduction and the volume averaged strain or stress of a cracked ply

for a given crack density. The study on the opening will extend to consider the delamination and matrix cracking together. For example, the amount of opening is directly influenced by the delamination length. As far as the opening due to delamination and matrix crack is involved, there is no work reported in the literature.

In order to understand delamination growth from crossing matrix cracks, a computational model for strain energy release rate calculation will be developed. Some researchers [16-18] have studied delamination near the crossing cracks. However, they considered only cross-ply laminates and did not perform a parametric study to determine the effects of various parameters on the strain energy release rates.

In this paper, our progress in developing a predictive model will be summarized. Our efforts will focus on three areas. The first is determining the effect of laminate design on opening of transverse matrix cracks and delaminations. Quasi-3D and fully three-dimensional finite element models were used to determine the effect of parameters such as loading, stacking sequence, and material properties on opening of the leakage path. As an example, Figure 1 shows a typical configuration of an angle ply laminate with transverse matrix cracks in each ply. The cracks are shaded in two of the plies. Two of the other variations studied include configurations with only one cracked ply or delamination at the intersection of transverse matrix cracks. The second area is experimental characterization and development of predictive models for initiation and evolution of damage during thermomechanical cycling. The loading currently consists of various sequences of uniaxial mechanical load combined with change in temperature from room temperature down to that for liquid nitrogen. Figure 2 shows a typical micrograph of a laminate with cracks which are microscopic and sparse. The third area is three-dimensional description of the damage state for laminates with known permeability. This last area has required the evaluation and development of destructive and non-destructive techniques for detecting the damage. Optical microscopy, x-radiography with various dye penetrants, and several ultrasonic NDE techniques are being explored.

The studies in these areas will be integrated to build analytical models that predict the effect of various parameters on permeability. The following sections describe progress in analytical and experimental studies including destructive and non-destructive techniques.

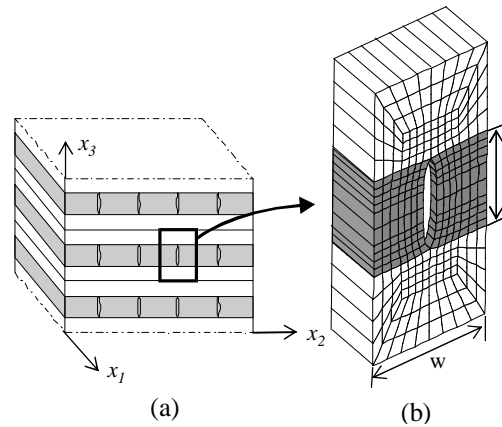


Figure 3. Modeling a laminate with transverse matrix cracks (TMC).

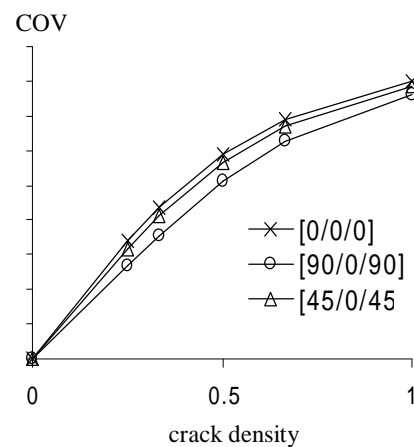


Figure 4. Effect of adjacent ply orientation and crack density on effective modulus E_{22} and crack opening volume (COV).

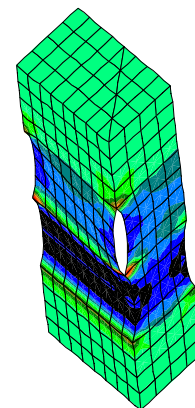


Figure 5. FEM Modeling of $[90/0_c/45_c/90]$ laminate with transverse matrix cracks in multiple plies.

ANALYSIS OF DAMAGE

In this section, we will describe progress in developing models to predict the initiation, evolution, and opening of damage. Most of the analytical work for formation of damage was on transverse matrix cracks. However, initial studies were conducted and are continuing to determine the interaction of transverse matrix cracks and delaminations. There were also some experimental studies of damage formation. The discussion of the development of the experimental equipment and the results are discussed later.

In order to simulate cracks occurring in laminates a finite element model for a representative volume element (RVE) was built. The RVE (or unit cell) is defined herein as the smallest region that represents the behavior of the entire region without any mirroring or rotation transformations. Figure 3(a) shows a laminate with matrix cracks, which are idealized based on the assumptions that the cracks are parallel to the x_1x_3 -plane and extend through the entire length and thickness of the ply. The cracks are also assumed to be periodically distributed. Due to the assumptions, periodic boundary conditions are applied to the RVE. The RVE with one crack is extracted from the laminate. A finite element mesh was built for this RVE as shown in Figure 3(b). It has been shown in the previous work that the degree of degradation of a cracked laminate is directly related to the crack opening displacements [19]. Hence, the understanding developed in the extensive parametric studies performed earlier by numerous researchers to determine the effective properties can be re-interpreted using formulas developed in Reference 11 to obtain insights about opening displacements, which are of great interest to this work. One major question addressed was whether the laminate stacking sequence can be designed such that when a crack does form, the opening is minimized. This is discussed next.

It is assumed that the x_2 direction is oriented perpendicular to the crack faces. The crack opening volume (COV) can be obtained from the u_2 displacements of the crack faces. In particular, the COV is defined to be

$$COV = \int_{CS} u_2 n_2 dS \quad (1)$$

where CS denotes the crack surface. Reference 19 derived the following formula to calculate the crack opening volume (COV) for a laminate based on the degradation of the E_{22} of a cracked lamina.

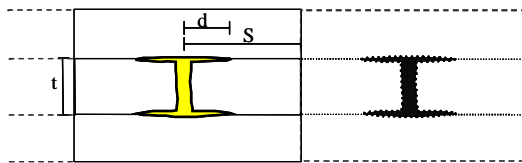


Figure 6. Modeling of delamination at crack tips

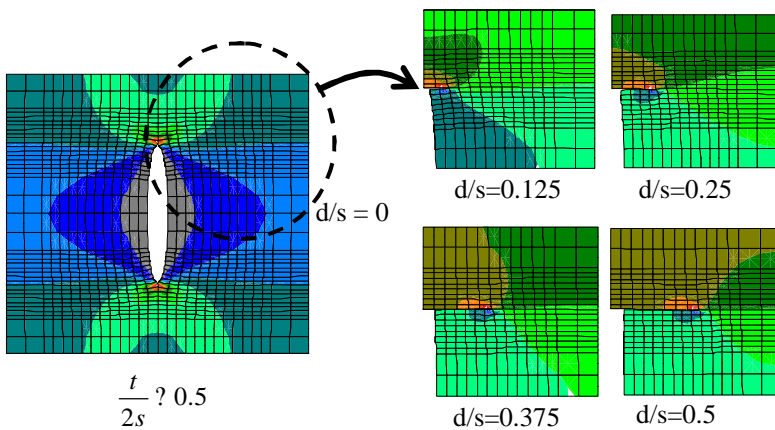


Figure 7. Effect of delamination length on deformation.

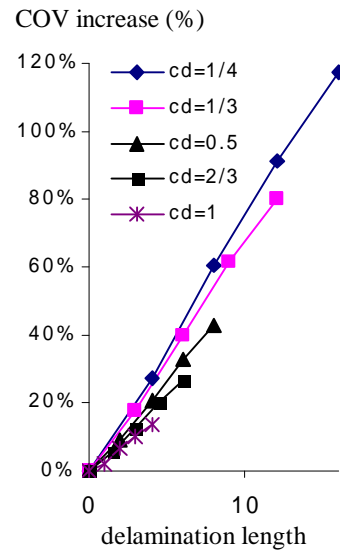


Figure 8. COV increase vs. delimitation length

$$COV = V \frac{\langle \bar{S}_{22} \rangle}{S_{22}} \frac{\langle \sigma_2 \rangle}{\langle \sigma_4 \rangle} \frac{\langle S_{24} \rangle}{S_{24}} \frac{\langle \sigma_4 \rangle}{\langle \sigma_2 \rangle} \quad (2)$$

where V , \bar{S}_{22} , and $\langle \sigma_2 \rangle$ are the volume, the effective compliance, and the volume averaged stress σ_2 of a cracked lamina, respectively. This formula can be approximated by

$$COV = V \frac{1}{\bar{E}_{22}} \frac{1}{E_{22}} \langle \sigma_2 \rangle \quad (3)$$

where the \bar{E}_{22} is the degraded E_{22} of a cracked ply. Figure 4 shows crack opening volume for three laminates with various crack densities in the middle lamina. The results suggest that the crack opening volume is not very sensitive to the laminate design. The COV was also calculated for $[0/90_c/0_c/90_c/0]$ and $[90/0_c/45_c/90]$ laminates with transverse matrix cracks in multiple plies. The deformed FEM mesh for $[90/0_c/45_c/90]$ is shown in Figure 5. The contour shows the variation of σ_{22} . The COV calculation based on Eqs. 2 and 3 were in very good agreement with FEA results. A more detailed description of this work can be found in Reference 19.

Microcracking can lead to other forms of damage such as delamination. Whether delaminations form and their size will greatly affect how easily fuel can pass through the maze of cracks. Laminate design may have a significant affect on the delamination initiation. A study is also being performed for delaminations that can form near the matrix crack tip (Figure 6). In Figure 6, t , s , and d are the thickness of the cracked ply, the transverse matrix crack spacing, and one-half of the delamination length, respectively. In this model, by changing the s and d , one can obtain different transverse matrix crack densities and delamination lengths. The opening displacement for this model has been studied. Figure 7 shows FEM meshes for the delamination near transverse matrix crack tips. In this FEA, the t and s were held constant as the delamination length d increases. Displacement boundary conditions were imposed to obtain $\langle \sigma_{22} \rangle = 1\%$. As shown in Figure 7, the opening increases with the delamination length. The effect of delamination length on the effective properties of the entire laminate with the middle cracked ply was examined. The study showed that degradation of E_{22} , G_{23} , G_{13} , and E_{33} of the laminate is very sensitive to the delamination. By assuming that the transverse matrix cracking and delamination affect only the properties of the middle ply, the reduced properties of the middle ply can be obtained. The additional E_{22} reduction of the middle ply due to delamination at the matrix crack was calculated. The laminates $[0/0/0]$, $[45/0/45]$, and $[90/0/90]$ with the different crack densities (.25-1.0) were analyzed to examine the effect of adjacent ply orientation and the crack density. It was found in the study that the E_{22} reduces almost linearly with the delamination length. The E_{22} reduction due to the delamination can be determined using FEA or a localization formula which is based on the homogenization formula presented in Reference 20. Also, a simple formula based on strength of materials was developed to calculate the E_{22} reduction. The results based on the localization and simple formulas were compared with the results by FEA and a good agreement was obtained. The FEM calculation for the increase of crack opening due to delamination is shown in Figure 8.

A simple relationship for average strain energy release rate associated with pop-in of transverse matrix cracks was developed and verified. The strain energy release rate for matrix cracking can be obtained easily for a displacement controlled case since the strain energy release rate is calculated using only the strain energy W (i.e. the work of the surface tractions is zero). The strain energy is $W = 1/2 \langle \sigma_i \rangle \langle \epsilon_i \rangle V$ where $\langle \rangle$ indicates the volume averaged

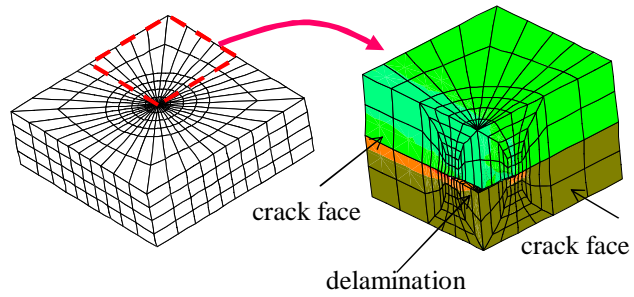


Figure 9. Modeling of delamination at the intersection of cracks.

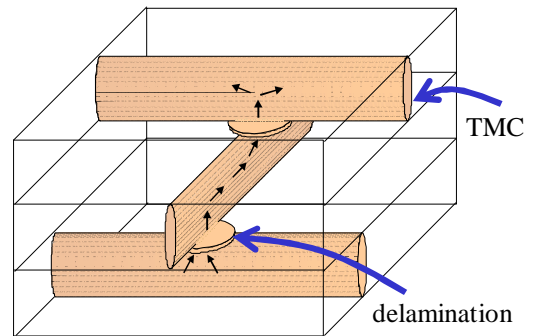


Figure 10. Network of matrix cracks and delaminations

value over a volume V . The strain energy can be rewritten as $W = \frac{1}{2} \bar{S}_{ij} \langle \sigma_j \rangle \langle \sigma_i \rangle V = \frac{1}{2} \bar{C}_{ij} \langle \epsilon_j \rangle \langle \epsilon_i \rangle V$. The effective stiffness matrix \bar{C} and compliance matrix \bar{S} of the laminate can be determined as a function of crack density using the modulus degradation for a middle cracked ply and homogenization techniques. Therefore, for given volume averaged strain or stress information, the strain energy and the strain energy release rate can be determined. The understanding developed in the parametric studies performed earlier to determine the effective properties can be re-interpreted using the formulas developed herein to obtain insights about strain energy release rate. This analysis helps understand whether the laminate stacking sequence can be designed such that cracks are prevented from occurring. It was found in the study that the strain energy release rate is sensitive to the type of loading but not very sensitive to adjacent ply orientation. This is expected since the strain energy depends on only the modulus degradation behavior and the volume averaged stresses and strains. Therefore, the strain energy release rate and the modulus degradation rate must show the same pattern. The results imply that the laminate stacking sequence does not much affect the resistance of the material to transverse matrix crack initiation and growth during service. Of course, stacking sequence can affect the stress state within a lamina, which is very important in determining the damage state. It has been known for a long time that delaminations often initiate at intersections of transverse matrix cracks [21].

The strain energy release rate for a delamination at the intersection of matrix cracks (Figure 9) was also calculated. Figure 9 shows a finite element model with a circular delamination at the crossing matrix cracks. The strain energy release rate has been calculated for various stacking sequences for circular delaminations. Future efforts will explore other delamination shapes which are more realistic. The opening due to matrix cracks and the delamination at the crossing matrix cracks is currently being investigated. Finite element models were developed and analyzed under axial and biaxial loadings. Further work is needed to examine the effect of various parameters such as delamination shapes (circle or ellipse...) and stacking sequence.

Parametric studies of the effective permeability are in progress based on models that consist of matrix cracks and delaminations (Figure 10).

EXPERIMENTAL CHARACTERIZATION

Experimental results are needed to verify the FEA models described in the above section. In this section, the experimental work on characterization of damage developed during thermomechanical cycling of cryogenic composite laminates will be discussed. Some researchers [2-5] have studied the damage evolution of cryogenic composites by applying different types of thermomechanical loading. Thermal loading usually consists of cycling between room or a higher temperature and a cryogenic temperature (most often liquid nitrogen, i.e. -196°C). Mechanical loading typically takes place at cryogenic temperatures, with an applied maximum stress level being a portion of the ultimate strength. In this section, combined thermal cyclic loading (room temperature to -196°C) and mechanical loading at -196°C and room temperature are performed on IM7/977-2 composite laminates. More specifically, thermal cycling (room temperature to -196°C) in the absence of mechanical load, thermal cycling followed by mechanical cycling at room temperature, and mechanical cycling at cryogenic temperatures are the three loading paths that have been investigated.

A high density polyethylene cryogenic dewar was used for the thermal cycles and an MTS 880 Materials Test System was used for the mechanical loading of the composite laminates tested at both room and cryogenic temperatures. Figure 11 shows the custom designed cryogenic chamber, which was mounted on the MTS 880 frame. The chamber was built of stainless steel, since steel has a relatively low thermal conductivity at cryogenic temperatures. An aluminum foil insulator was added around the chamber in order to improve insulation. A sealant was used to avoid leakage from the bottom of the chamber. After the sealant was cured at room temperature for 36 hours, the chamber was filled with liquid nitrogen. The composite specimens were held for 30 minutes in liquid nitrogen to guarantee that they had reached the same temperature as liquid nitrogen. Subsequently, the specimens were mechanically loaded while still being held in the liquid nitrogen. During the mechanical loading, the stress and strain values were obtained. The strain values were calculated by using the cross-head displacement, while the stress values were determined from a load cell attached on the cross-head.

After two thermal or mechanical cycles, the specimens were examined using an optical microscope to collect damage state information, such as crack density for each ply and delamination length occurring at interfaces between plies.

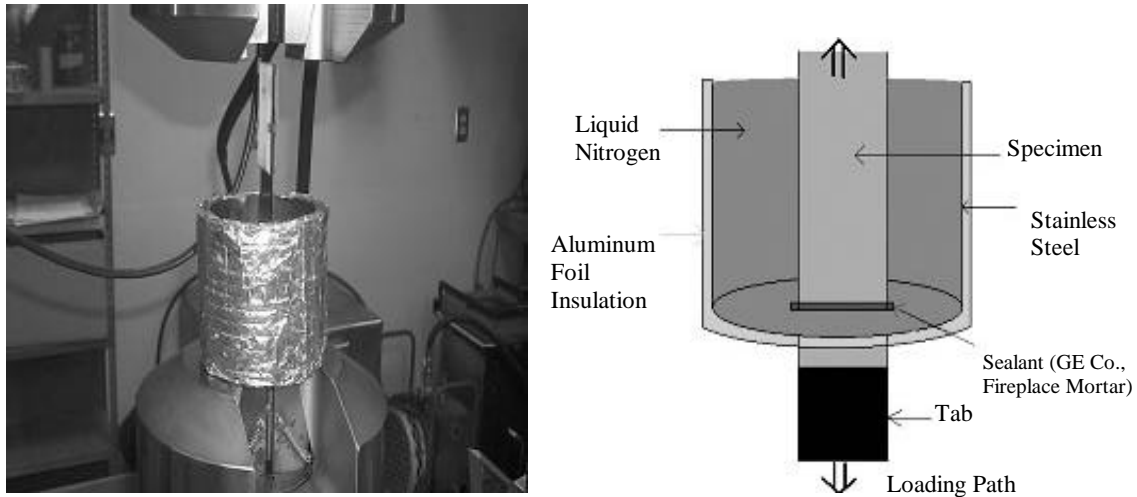


Figure 11. Cryostat system mounted on an MTS 880 frame

The specimens tested were provided by Lockheed Martin, and they were 18-ply graphite epoxy IM7/977-2 laminates with $[0/-45/90/45/0/45/90/-45/0]_s$ stacking sequence, and with dimension of 11.75" X 3.5". The specimens had undergone prior thermomechanical testing, including thermal cycles from room temperature to liquid Nitrogen (-196°C) and mechanical cycles at cryogenic temperatures (-196°C). From the specimens received, several were tested under additional thermomechanical loading, and others were tested nondestructively for the evaluation of their damage state. For the thermomechanical loading tests, the original specimens were cut into three pieces, as indicated in Figure 12.

First, a laminate specimen was mechanically tested at room temperature in uniaxial tension to failure in order to determine the Young's modulus and ultimate tensile strength. The Young's modulus and ultimate tensile strength were determined to be 61.2 GPa and 787.02 MPa, respectively. Then, a second laminate that had undergone four mechanical and thermal cycles, was cut into three pieces from the original specimen shown in Figure 12, and machined with a dimension of 10" x 1" according to ASTM standards, D3039/3039M-00 recommendation.

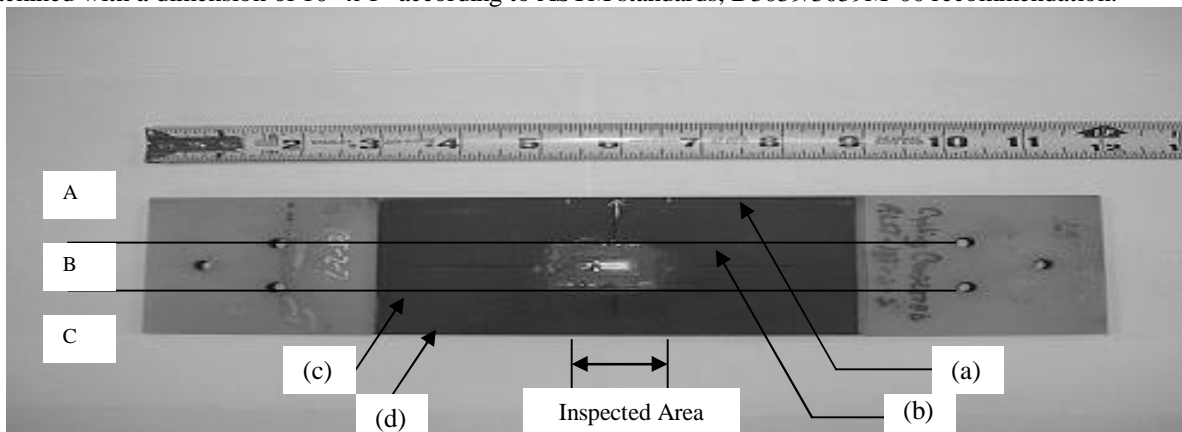


Figure 12. Cryogenic composite laminate - IM7/977-2

The three resulting specimens, indicated as A, B, and C in Figure 12, were characterized for damage before any loading cycle was applied. Cracks were counted in each non-zero degree ply along a 1.26" (32 mm) span centered lengthwise on each specimen. Specimen A underwent a total of 20 thermal cycles. Specimen B was subjected to 2 thermal cycles followed by 2 mechanical cycles at 60% of the ultimate tensile strength at room temperature. The 4 cycles were repeated three times, and the specimen was inspected after each mechanical and thermal loading cycle. Mechanical loading at cryogenic temperatures was applied to specimen C, but the test was terminated early due to delamination reaching the grips.

Figure 13 shows the crack densities of the second ply from the outer surface [-45], and their increase with the number of loading cycles for specimens A, B, and C, respectively. Similar trend in the rate of crack density growth has been observed in the third ply [90] of the specimens tested. The zero in the horizontal axis defines the initial

state of each specimen, while each cycle on the graph corresponds to two physical cycles, either mechanical or thermal. When thermal cycles (specimen A) alone were applied, there were no additional cracks in the material up to 20 cycles. However, thermal cycling, followed by mechanical cycling at room temperature (specimen B), resulted in a rapid increase of microcracking induced damage, which saturated after it reached a level of about eight times the initial damage. Even higher rate of increase of damage densities were observed in specimen C, which was mechanically cycled at cryogenic temperatures, but delamination at the grips resulted in termination of the experiment.

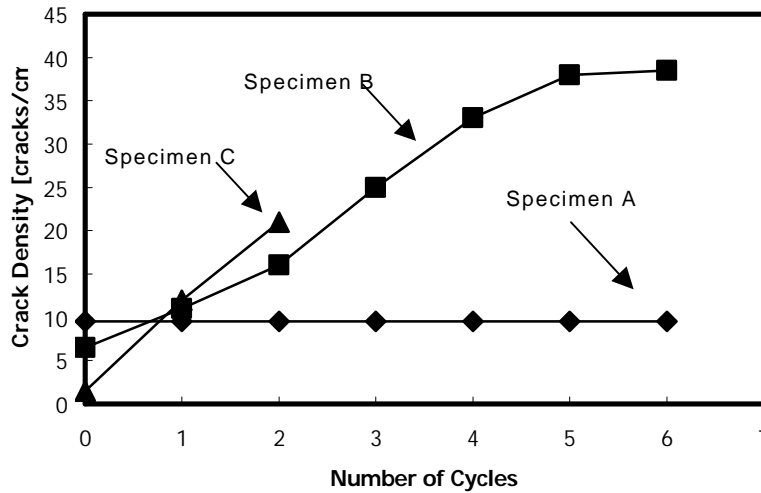


Figure 13. Micro-crack density versus number of cycles for the $[-45]$ ply (second from outer surface)

Figure 14 shows typical optical micrographs taken in the middle of the specimen edge at the end of the loading cycles. The initial damage state, which is the damage of specimen A is shown in Figure 14(a). The damage state after twelve loading cycles for specimen B and four mechanical cycles for specimen C are shown in Figure 14(b) and 14(c), respectively. Cracks were found only in plies 2, 3, and 4 in the $[0/-45/90/45/0/45/90/-45/0]_s$ laminate. This is an unusual case, and a possible cause can be due to the presence of residual stresses resulting from manufacturing process or stress concentrations at micro cracks in the above plies.

Delaminations were observed between plies 2,3, and 3,4. The majority of the interface cracks were observed between plies 2,3, as shown in Figure 14(c). From the above results, one can conclude that for simultaneous mechanical loading in a cryogenic environment, the chances of delamination and hence leakage is higher than thermal testing followed by mechanical loading at room temperature. Delaminations at transverse crack tips were also observed, which could be more critical for the permeability and leakage problem.

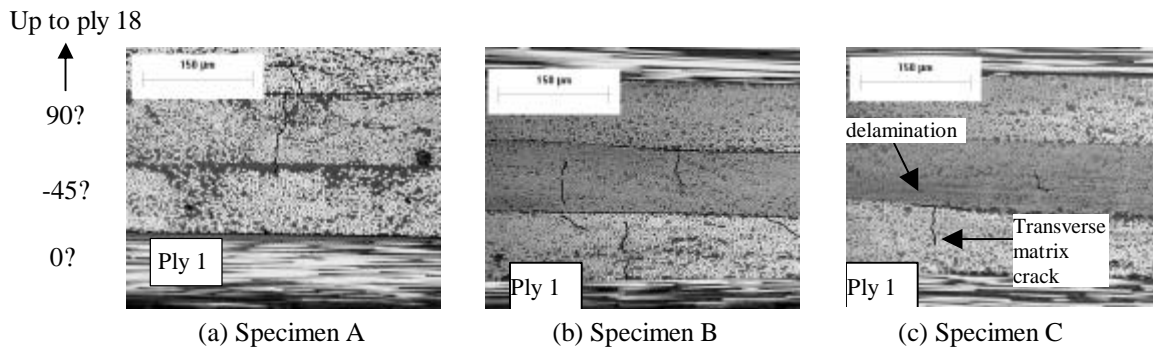


Figure 14. Micrographs showing damage after testing

Additional loading conditions such as thermal cycling at constant load and also variable mechanical load are being planned for cryogenic composite laminates with an undamaged initial state. This would facilitate the verification of loading condition importance in damage development. Also, the influence of thermal gradients on damage development will be investigated, as specimens are brought to cryogenic conditions. Such large temperature

variations through the thickness may result in thermal stresses and possible delaminations at the interfaces. The influence of thermal gradients on damage development will be investigated both experimentally and numerically, using a FEA model. In future work, thermomechanical loading tests will be accompanied by a concurrent nondestructive evaluation of damage; these NDE techniques are described next.

PLY-TO-PLY DETERMINATION OF DAMAGE

In the following, we briefly discuss salient features of these NDE techniques (optical edge examination, X-ray radiography and ultrasonics) for a ply-by-ply determination of damage.

Optical Examination of Edges

Edges of each specimen were polished progressively using 600 and 1200 grit sandpapers and then using high purity 0.3 μ m alumina powder to get a near optical-quality finish. Edge cracks were mapped using an optical microscope (200X magnification) equipped with a motorized positioning stage controlled by a computer. The recorded data files were later used to generate crack map (schematics), which were subsequently compared with images obtained from X-ray and ultrasonic examinations. Though optical examination of edge cracks provides one of the simplest forms of damage evaluation and is fairly reliable (doubtful places can be reexamined at higher magnification), it fails to provide any information regarding the extent to which cracks have propagated through the width of a laminate. In other words, optical examination cannot provide any information about the extent of partial cracks (cracks that appear only at one of the two edges) or the presence of internal cracks (cracks that do not appear on any of the edges); such cracks were found very frequently in the laminates tested. As an example, one of the 18-ply graphite epoxy IM7/977-2 specimens mentioned in the previous section was cut into three pieces (as shown in Figure 12) and the edge cracks in the 3rd [90] ply were examined. The resulting damage densities are presented in Figure 15 for the edges indicated in Figure 12. This specimen underwent thermomechanical testing at cryogenic temperatures, similar to the specimens tested in the previous section, and in addition a Helium leak testing was also performed. A careful examination of this data revealed that a vast majority of the cracks do not traverse the entire width of the specimen.

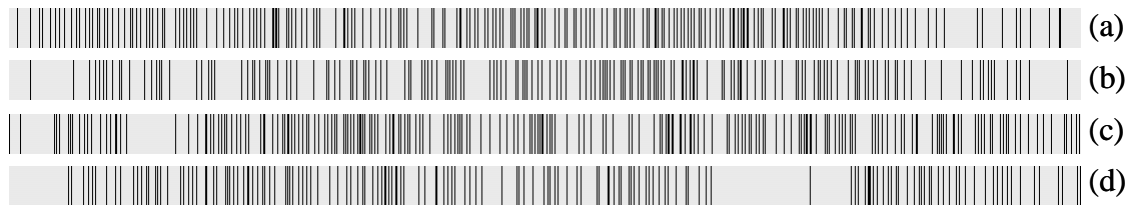


Figure 15. Relative crack position in 3rd [90] ply of 3.6'' wide 18-ply [0/-45/90/45/0/-45/90/45/0]_s laminate at specimen edges (a),(d) and at cuts at 1.2'' (b) and 2.4'' (c) distance from edge (a).

X-Ray Radiography

Penetrant enhanced X-ray radiography is one of the most widely used techniques for damage characterization, and frequently considered the best NDE technique available for imaging the crack distribution in composite. With the use of a proper contrasting agent (in the present case, diiodomethane [22]), a clear picture of matrix cracks is seen as dark lines in the X-ray images (see Figure 16). This has been further confirmed by a comparison of X-ray images with optical and ultrasonic techniques. A part of the X-ray image of matrix cracks in highly damaged 8-ply laminate, is presented in Figure

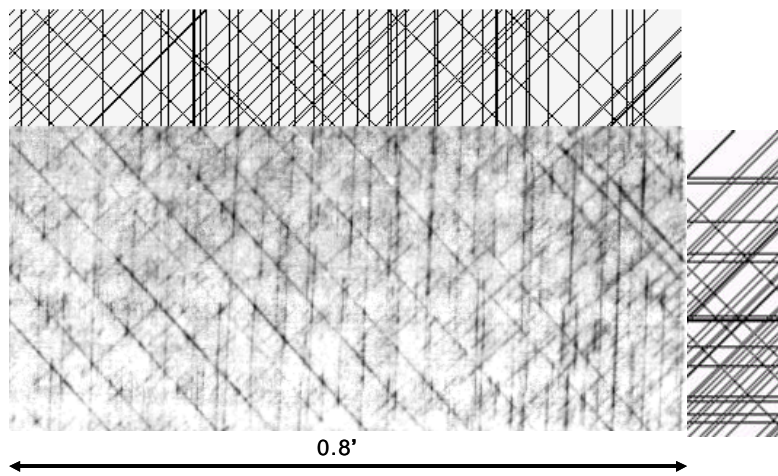


Figure 16. A comparison of a part of the X-ray image of the 8-ply, [90/45/0/-45]_s, laminate with a schematic of optically detected matrix cracks (top and right side of the picture).

16. At the top and the side of the figure, a schematic of the optically detected edge cracks is plotted. Cracks found in 90° plies are plotted as vertical lines, cracks found in 45° plies are plotted as lines at 45° , and so forth. Fairly good correlation of the position of dark lines in the figure with the schematic of the optically detected matrix cracks confirms that the dark lines which look like cracks in the figure are indeed matrix cracks. However, as is well known, an X-ray image is a 2-D projection of the damage, which makes ply-by-ply damage evaluation difficult. In a real life situation where one does not have access to the composite edges the techniques becomes inapplicable. Moreover, it is not a “true” nondestructive technique because of possible specimen degradation by the penetrant.

Ultrasonics

The laminates were tested extensively using different ultrasonic techniques and transducer combinations. These include through-transmission, scattering in transmission (pitch-catch), and polar backscattering for detection of matrix cracks. The standard pulse-echo C-scan technique was used to detect delaminations. By appropriately time-gating the output signals, it was found possible to carry out a ply-by-ply examination.

Polar backscattering technique, i.e. scattering of ultrasound by crack and ply boundary back toward inclined transducer, using a spherically-focused, 25-MHz transducer was found to be the best technique for imaging matrix cracks including internal cracks [23,24]. In this technique a single transducer is used as a transmitter and receiver. The signal-to-noise ratio was found to be rather high (in some cases more than 30 dB) indicating a high level of confidence of detection.

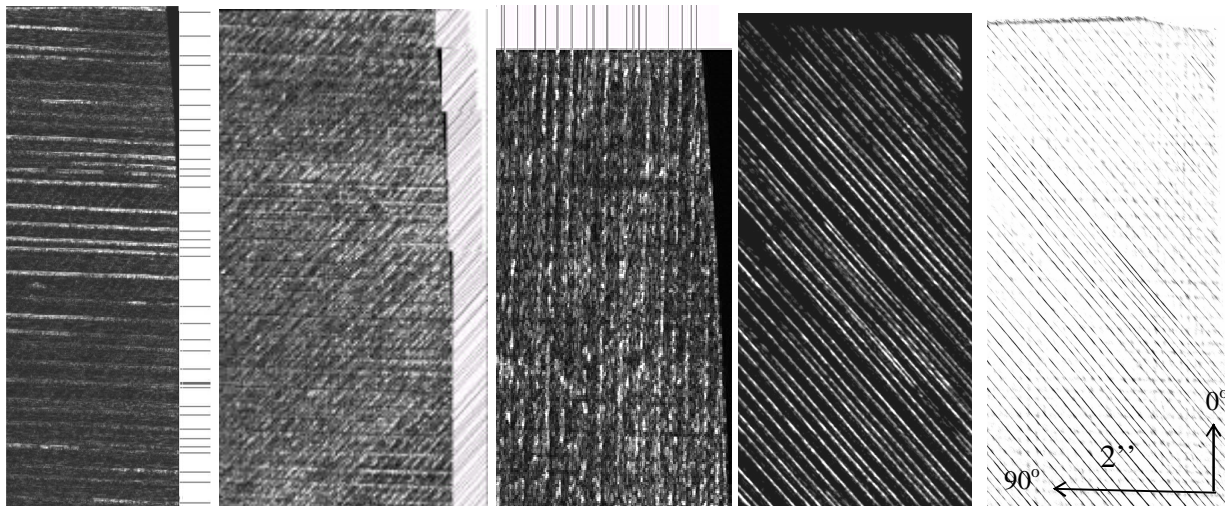


Figure 17. From left to right: Ultrasonic images of 1st, 2nd, 3rd, and 4th plies, and filtered X-ray images of cracks in the 4th ply of the 8-ply, $[90/45/0/-45]_s$, specimen.

A comparison of the ultrasonic (polar backscattering) and X-ray (filtered to remove lines in all other directions) images of the second ply of the 8-ply specimen is presented in Figure 17. An excellent correlation can be seen between them. Moreover, both the images correlate well with optical edge crack detection results. The information obtained from the aforementioned NDE techniques is complementary to each other and a high degree of reliability can be achieved in damage characterization with a judicious combination of all three techniques.

CONCLUDING REMARKS

Optimal design of composite cryogenic tanks requires an analysis that can predict microcracking induced permeability. The current work is focused on laying the foundation for such an analysis. This requires a combination of parametric analytical and experimental studies and development of techniques to determine the 3D distribution and connectivity of damage. This paper briefly described progress in these areas.

ACKNOWLEDGEMENT

This work was supported by NASA through the National Center for Advanced Manufacturing Louisiana

Partnership, Grant # NCC8-223. Any opinions, findings, and conclusions or recommendations expressed in this material are those of the authors and do not necessarily reflect the views of the National Aeronautics and Space Administration.

REFERENCES

1. D.S. Adams, D.E. Bowles and C.T. Herakovich. "Thermally Induced Transverse Cracking in Graphite/Epoxy Cross-Ply Laminates," *Journal of Reinforced Plastics and Composites*, Vol. 5, July, pp. 152-169. 1986.
2. S.S. Kessler, T. Matuszeski and H. McManus. "Cryocycling and Mechanical Testing of CFRP for the X-33 Liquid H₂ Fuel Tank Structure," *Proceedings of the American Society for Composites (ASC)*, Sept. 9-12, 2001, Virginia Tech, Blacksburg.
3. R.Y. Kim, S.L. Donaldson, "Experimental Observation of Microcracking of Composite Laminates under Cryogenic Temperature", AIAA, Aug., 28-30, 2001.
4. V.T. Bechel, M.B. Fredin, and S.L. Donaldson. "Combined Cryogenic and Elevated Temperature Cycling of Carbon/Polymer Composites", Society for the Advancement of Materials and Process Engineering, Long Beach, CA, May 2002.
5. S.L. Donaldson, R.Y. Kim, "Fatigue of Composites at Cryogenic Temperature", Society for the Advancement of Materials and Process Engineering, Long Beach, CA, May 2002
6. H.K. Rivers, J.G. Sikora, and S.N. Sankaran, "Detection of Micro-Leaks Through Complex Geometries under Mechanical Load and at Cryogenic Temperature," AIAA 2001-1218.
7. H.L. McManus and J.R. Maddocks, "On Microcracking in Composite Laminates under Thermal and Mechanical Loading," *Polymers and Polymer Composites*, Vol. 4, No. 5, 1996, pp. 304-314.
8. H.L. McManus, A. Faust, and S. Uebelhart. "Gas Permeability of Thermally Cycled Graphite-Epoxy Composites," *Proceedings of the American Society for Composites (ASC)*, Sept. 9-12, 2001, Virginia Tech.
9. H. Kumazawa, T. Aoki, T. Ishikawa, and I. Susuki. "Modeling of Propellant Leakage Through Matrix Cracks in Composite Laminates," AIAA-2001-1217.
10. T. Yokozeki, T. Aoki, and T. Ishikawa. "Transverse Crack Propagation Process across the Specimen Width in Toughened CFRP Laminates," AIAA-2001-1639.
11. J. Noh and J. Whitcomb. "Effect of Various Parameters on the Effective Properties of a Cracked Ply," *Journal of Composite Materials*, Vol. 34, 2001.
12. Z. Hashin. "Analysis of Cracked Laminates: A Variational Approach," *Mechanics of Materials*, 4:121-136, 1985.
13. J.A. Nairn. "Some New Variational Mechanics Results on Composite Micro Microcracking," *Proc. 10th Int. Conf. on Comp. Mat.*, Whistler, B.C., Canada. 110, 1995.
14. G.J. Dvorak, N. Laws, M. Hejazi. "Analysis of Progressive Matrix Cracking in Composite Laminates I. Thermoelastic Properties of a Ply with Cracks," *Journal of Composite Materials*, 19: 216-234, 1985.
15. P. Gudmenson, and W. Zang. "An Analytical Model for Thermoelastic Properties of Composites Laminates Containing Transverse Matrix Cracks," *International Journal of Solids and Structures*, 23: 1301-1318, 1993.
16. R.D. Jamison. "Advanced Fatigue Damage Development in Graphite/Epoxy Laminates," Ph.D. Dissertation, College of Engineering, Virginia Polytechnic Institute and State University, 1982.
17. A.S. Wnag, N.N. Kishore and C.A. Li. "Crack Development in Graphite-Epoxy Cross-ply Laminates under Uniaxial Tension," *Composites Science and Technology*, 24, 1-31, 1984.
18. J. Whitcomb. 1992. "Analysis of Delamination Growth near Intersecting Ply Cracks," *Composite Journal of Composite Materials*, Vol. 26, No. 12, pp. 1844-1858, 1992.
19. J. Noh and J. Whitcomb. "Effect of Laminate Design and Loads on Crack Opening Volume in Laminates Used in Cryogenic Tanks," *Proceedings of 43rd AIAA/ASME Structures, Structural Dynamics and Materials Conference*, Denver, April, 2002.
20. J. Whitcomb and J. Noh. "Concise Derivation of Formulas for 3D Sublaminate Homogenization," *Journal of Composite Materials*, 34(6):522-535, 2000.
21. A.L. Highsmith, and K.L. Reifsnider "On Delamination and the Damage Localization Process," *AMD, ASME*, 74:71-87.
22. E.A. Birt, "The application of X-radiography to the inspection of composites," *INSIGHT* Vol 42, No. 3, pp. 151-157, 2000.
23. K. Maslov, R. Kim, V. Kinra, N. Pagano. "A new technique for the ultrasonic detection of internal transverse cracks in carbon-fibre/bismaleimide composite laminates," *Composite Science and Technology*, Vol. 60, pp. 2185-2190, 2000.
24. K. Steiner, R. Eduljee, X. Huang, J. Gillespie Jr. "Ultrasonic NDE techniques for the evaluation of matrix cracking in composite laminates", *Composite Science and Technology*, Vol. 53, pp. 193-198, 1995.